Orbital magnetic moments of Co in multilayers with perpendicular magnetic anisotropy

D. Weller, Y. Wu, J. Stöhr, and M. G. Samant
IBM Research Division, Almaden Research Center, 650 Harry Road, San Jose, California 95120

B. D. Hermsmeier
IBM San Jose, 5600 Cottle Road, San Jose, California 95153

C. Chappert
Institut d'Electronique Fondamentale, Batiment 220, Université Paris-Sud, 91405 Orsay, France
(Received 29 June 1993; revised manuscript received 14 December 1993)

The out-of-plane orbital magnetic moment of Co in Co/X multilayers (X=Pd, Pt and Ni) with perpendicular magnetic anisotropy has been investigated using x-ray magnetic-circular-dichroism spectroscopy. The orbital d moment per Co atom, $m_{\mathrm{orb}}^{\perp}$, is considerably enhanced by $(0.15\pm0.02)\mu_B$ and $(0.07\pm0.02)\mu_B$ in Co/Pd and Co/Pt multilayers, respectively, compared with a single thick Co film. No respective enhancement is found in the case of Co/Ni. This enhancement does *not* scale with the spin-orbit coupling parameter ξ_{SO} of Ni-3d, Pd-4d, and Pt-5d bands despite strong d-d mixing which leads to the presence of ferromagnetic moments of Pd and Pt atoms. However, a roughly linear scaling relation of the out-of-plane orbital moment $m_{\mathrm{orb}}^{\perp}$ with the intrinsic uniaxial anisotropy constant $K_{u,1}^{\mathrm{Co}}$ per Co volume is observed. This experimental finding is interpreted in conjunction with recent *ab initio* and tight-binding band-structure calculations as evidence for a preferential enhancement of the out-of-plane orbital moment of Co in Co/Pd and Co/Pt multilayers.

I. INTRODUCTION

Metallic multilayers of the type Co/X (=Pt, Pd, Au, Ni, Ir,...) are a novel class of magnetic thin film materials with several unique properties, which makes them interesting for magnetic and magneto-optic recording applications. The phenomenon of perpendicular magnetic anisotropy is of particular importance. It has phenomenologically been explained by an extra anisotropy energy contribution due to symmetry break at internal interfaces.[1,2] Microscopically, this interface anisotropy energy has recently been calculated from *first principles* and attributed to magnetocrystalline anisotropy.[3,4] In essence, magnetocrystalline anisotropy arises from the spin-orbit interaction. This interaction causes the existence of an orbital moment which is anisotropic with respect to the crystal axes, and it also leads to an alignment of the spin moment with the orbital moment. The resulting anisotropy of the total magnetic moment is reflected in the dependence of the total energy on the orientation of the magnetic moment. In the itinerant ferromagnets Fe, Co, and Ni the orbital magnetic moment is largely quenched due to crystal field interactions[5] and its value is only about 10% of that of the spin moment.[7,8] It is also only weakly anisotropic with respect to the crystal axes.[6] This situation is different in ultrathin films and multilayers, where *enhanced* anisotropic orbital moments have been predicted first in tight-binding[9] and more recently in *ab initio* calculations.[3,4] However, there is considerable controversy in these theories about the exact quantitative values of the orbital moments, which may vary by more than a factor 2, depending on the details of the band-structure calculation and, in particular, on the inclusion of an extra orbital polarization term, which is apparently needed to explain the experimentally well-known orbital moment of bulk Co.[3,10–13] First experimental evidence of a considerable enhancement of the average orbital magnetic d moment of Co atoms in a Co/Pd multilayer was recently reported by us using the method of x-ray magnetic circular dichroism (XMCD) spectroscopy.[14] Here we extend our previous study to Co/Pt and Co/Ni multilayers and, more importantly, address the correlation between the orbital moment enhancement in the direction perpendicular to the film plane and the uniaxial anisotropy in these systems.

II. SAMPLE PREPARATION

The structures under investigation were 20 ×[Co(2 Å)/Ni(4 Å)], 20×[Co(2–8.5 Å)/Pd(10 Å)], and 20×[Co(2–8.5 Å)/Pt(10 Å)] multilayers with large perpendicular remanence. All samples were deposited by e-beam evaporation from individual elemental metal sources on polished Si(100) wafers. The base pressure was 5×10^{-8} Torr with a typical pressure during deposition of 2×10^{-7} Torr. The deposition rates, typically 0.2 Å/sec for Co and 0.5–1 Å/sec for Pd, Pt, and Ni, and the thicknesses of the individual layers were monitored by quartz crystal oscillators. The temperatures during growth were kept below 80°C and the substrates were mildly etched (1 min, 10 mA, 100 eV, Ar^+) prior to the

deposition of Au, Pd, and Pt buffer layers, which are needed to control the texture and magnetic properties of the subsequently deposited multilayers. In the case of Co/Ni an additional 10 Å capping layer of Pd was employed. θ-2θ x-ray diffraction studies revealed that the present films are polycrystalline with a strong fcc(111) texturing axis along the film normal. From the width of the fcc(111) peak grain sizes of the order of ~ 100 Å are inferred. Rocking curve studies show a dispersion angle of the order of 15–20°. Additional x-ray fluorescence measurements were used to characterize the actual individual layer thicknesses which were found to be within 5% of the above-quoted nominal thicknesses. As a reference sample we used a 250 Å thick dc-magnetron sputtered Co film which showed close to 100% in-plane remanence as described earlier.[14]

III. MAGNETIZATION AND MAGNETIC ANISOTROPY

Magnetic properties were studied in detail using vibrating sample (VSM) and torque magnetometry as well as angle dependent Kerr loops. Room temperature magnetization data for the samples containing 2 Å Co were obtained from VSM hysteresis loop measurements with a field of up to 20 kOe aligned in the normal direction. These data, normalized to the total, Co plus spacer layer, volume are contained in the second column of Table I. We have also derived the magnetizations per Co volume ($M_S^{\rm eff}$ in column 3) and the contributions from Ni, Pd, and Pt (M_S^X in column 4) by assuming a magnetization profile according to $M_S D = \langle M_S^{\rm Co}\rangle d_{\rm Co} + \langle M_S^X\rangle d_X$. Here X refers to Ni, Pd, and Pt, respectively, $D = d_{\rm Co} + d_X$ is the bilayer period and $\langle M_S^{\rm Co}\rangle$ and $\langle M_S^X\rangle$ are the average magnetizations of the Co and X layers, respectively. By normalizing to the Co volume only we can determine the effective magnetization $M_S^{\rm eff} = M_S D/d_{\rm Co}$ and by setting $\langle M_S^{\rm Co}\rangle$ to its bulk value of 1400 kA/m we can determine the average spacer magnetizations $\langle M_S^X\rangle$. Both, the strongly enhanced magnetization per Co volume, $M_S^{\rm eff}$, and the average spacer magnetizations, $\langle M_S^X\rangle$ are in reasonable agreement with the known saturation magnetization of Ni (484 kA/m) (Ref. 15) and with the presence of spin polarized Pd and Pt atoms in these structures.[16,17,4] Table I furthermore includes in column 5 the demagnetization energies K_d, which were obtained in a similar fashion according to

$$K_d D = K_d^{\rm Co} d_{\rm Co} + K_d^X d_X$$

and

$$(K_d)^{X,{\rm Co}} = (-\tfrac{1}{2}\mu_0 M_S^2)^{X,{\rm Co}}\ , \tag{1}$$

i.e., assuming a homogeneous magnetization profile within the Co and X layers. We have generally assumed a constant saturation magnetization of $M_S^{\rm Co}$=1400 kA/m within the Co layers, which gives rise to a demagnetization contribution $K_d^{\rm Co} = -1.23$ MJ/m^3. While Eq. (1) presents a good approximation for the present Co/Ni multilayers, more realistic slab profiles, e.g., based on calculated magnetization profiles of Pt (Ref. 18) and Pd atoms[19] in contact with Co, could be used for the Pd and Pt spacer layers. Respective alterations of the profiles, e.g., by localizing 80% of the Pd and Pt moment within the first atomic layers adjacent to Co, however, would lead only to minor corrections for the quoted K_d values in Table I and have therefore been neglected.

The magnetic anisotropy of the present samples was determined using several independent methods. This is essential in order to reliably determine the anisotropy constants of a system.[20] Figure 1 first shows torque curves $L(\alpha)$ measured at room temperature in a constant field of 20 kOe for the Co/Ni, Co/Pd, and Co/Pt multilayers containing 2 Å Co. We use angle definitions as indicated in the inset and make the assumption that the free energy per unit volume of the system depends only on the angle θ between the normal direction $\mathbf{n}$ and the magnetization vector $\mathbf{M}$. In other words, we treat these multilayer films as uniaxial systems, with the [111] crystal axis parallel to the film normal direction $\mathbf{n}$. This is a reasonable assumption for the present fcc(111) oriented multilayers which showed negligible in-plane anisotropies—mainly of sample shape origin—of the order of 10 kJ/m^3 or smaller. Considering terms up to second order in $\sin^2\theta$ only, we can write

$$F = K_0 + K'_{u,1}\sin^2\theta + K_{u,2}\sin^4\theta, \tag{2}$$

where $K'_{u,1}$ is the effective first-order uniaxial anisotropy constant, which contains the demagnetization term K_d as defined in Eq. (1): $K'_{u,1} = K_{u,1} + K_d$. $K_{u,2}$ is the second-order uniaxial anisotropy constant and K_0 contains all angle independent energy terms. $K'_{u,1}$ and

TABLE I. Magnetic properties of Co(2 Å)/Ni(4 Å), Co(2 Å)/Pd(10 Å), and Co(2 Å)/Pt(10 Å) multilayers. Magnetizations are quoted in kA/m (emu/c.c.) and the anisotropy constants (K_d, $K'_\perp$, $K_\perp$) and Fourier components (L_2, L_4) are in units of MJ/m^3 (10^7 erg/c.c.). Energies and magnetizations are per Co plus spacer volume except for $M_S^{\rm eff}$ and M_S^X = Ni, Pd, Pt, which are quoted per Co and X (=Ni, Pd, and Pt) volume, respectively. The intrinsic uniaxial anisotropy constant $K_\perp$ was obtained by subtracting from the measured anisotropy energy $K'_\perp$ the demagnetization energy K_d, estimated from $K_d D = K_d^{\rm Co} d_{\rm Co} + K_d^X d_X$, i.e., by assuming uniform magnetization in the individual layers.

Structure	M_S	$M_S^{\rm eff}$	M_S^X	K_d	L_2	L_4	$K'_\perp$	$K_\perp$
Au(300)/20×[Co(2)/Ni(4)]	810	2430	515	-0.521	0.095	0.0207	0.107	0.628
Pd(200)/20×[Co(2)/Pd(10)]	360	2160	148	-0.216	0.348	0.111	0.61	0.826
Pt(200)/20×[Co(2)/Pt(10)]	310	1860	88	-0.207	0.200	0.053	0.31	0.517

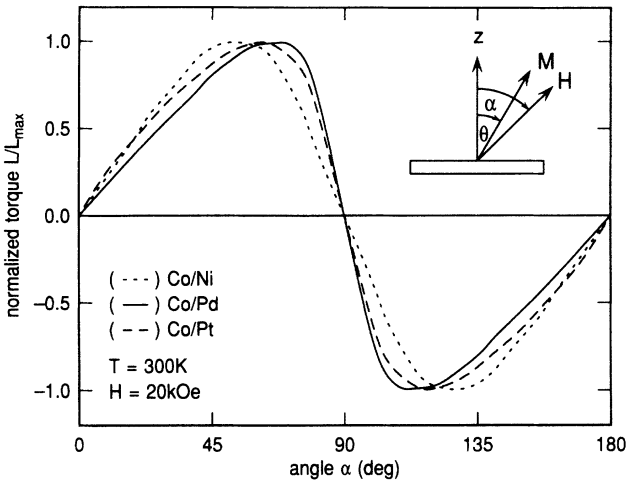

FIG. 1. Torque curves $L(\alpha)$, meausured at room temperature in a constant field of 20 kOe on 20 period Co(2 Å)/Ni(4 Å), Co(2 Å)/Pd(10 Å), and Co(2 Å)/Pt(10 Å) multilayers on Au, Pd, and Pt buffers (see text). α is the angle between the normal direction **n** and field direction **H** and θ denotes the angle between the normal direction **n** and magnetization vector **M**, as indicated in the inset.

$K_{u,2}$ can in principal be determined from angle dependent torque measurements if the external field is strong enough to keep the sample in a single domain state for all angles α of the field direction **H** with respect to the normal direction **n** of the sample. Thus in the case of $\alpha = \theta$, we obtain for the measured torque per unit volume

$$L(\alpha) = L(\theta) = -\frac{\partial F}{\partial \theta} = (K'_{u,1} + K_{u,2}) \sin 2\theta + \frac{K_{u,2}}{2} \sin 4\theta. \quad (3)$$

A Fourier analysis of the torque curves in Fig. 1 yields the sin2α and sin4α components L_2 and L_4, respectively. This analysis is shown in columns 6 and 7 of Table I. While the torque curves clearly demonstrate the perpendicular easy magnetization axis, the presence of a substantial L_4 component together with the observation of some rotational hysteresis (not shown) indicates that the present samples are not perfectly uniaxially aligned and that the applied field strength is insufficient to align the magnetization parallel to the external field for all angles α. We have therefore also measured field dependences of the torque at a fixed angle of $\alpha = 45°$ and determined the effective perpendicular anisotropy $K'_\perp$ by extrapolating to infinite field.[21] The symbol $K_\perp$ instead of $K_{u,1}$ is chosen to indicate the different method of measurement. In a truly uniaxial system with negligible higher-order anisotropies, both constants are the same. The respective results are shown in column 8 in Table I. We note, that in-plane magnetization measurements and a derivation of the perpendicular anisotropy using the area between the out-of-plane and in-plane loops gave consistent results, however, due to the large anisotropy fields of up to ~50 kOe in Co/Pd and the limited maximum field of only 20 kOe in these experiments, this method must be considered less reliable. The intrinsic first-order perpendicular anisotropy constant $K_\perp$ is obtained as $K_\perp = K'_\perp + K_d$. $K_\perp$ is largest for Co/Pd, intermediate for Co/Ni and smallest for the present Co/Pt multilayers.

Polar Kerr hysteresis measurements with the field aligned in the film normal direction are shown in Fig. 2. They show mainly square loop behavior with high coercivity and close to 100% remanence, confirming the magnetometry results. In Co/Pd and Co/Pt multilayers with thicker Co layers, the out-of-plane remanence was found to drop continuously to values of about 33% for the 8.5 Å thick Co layer. We have also carried out polar Kerr loop measurements with the field oriented at an angle α with respect to the normal direction. Figure 3 shows typical results obtained for Co/Ni ($\alpha = 20°$) and Co/Pd and Co/Pt ($\alpha = 60°$). The samples were first saturated at $\alpha = 0°$ using the maximum available field of +20 kOe, then the field was set back to zero and the sample was rotated to the desired angle α and finally a full polar hysteresis loop starting at H=0 was recorded. This method was earlier suggested by Haijar *et al.*[22] ($\alpha = 90°$ only) and has more recently been discussed in detail by Purcell *et al.*[23] in conjunction with Co/Pd(111) wedges. We note that the choice of the field angle α is crucial and that measurements at $\alpha = 90°$, i.e. with the field aligned within the plane of the film, do not generally allow to obtain information on the anisotropy constants. In general, α will have to be smaller for weaker anisotropy samples in order to avoid magnetization reversal due to domain formation. If applied appropriately, the Kerr technique allows to extract the anisotropy constants $K_{u,1}$ and $K_{u,2}$ with a spatial resolution given by the laser beam, which can be focused if necessary. It relies on the fact that in the polar Kerr geometry the measured Kerr angle is proportional to the normal component of the magnetization $M_n = M_S \cos(\theta_{eq})$, where θ_{eq} is the *equilibrium*

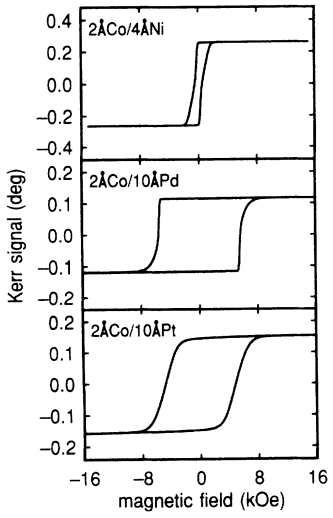

FIG. 2. Polar Kerr hysteresis loops (He-Ne laser) of the samples discussed in Fig. 1. For hysteresis properties see Table II.

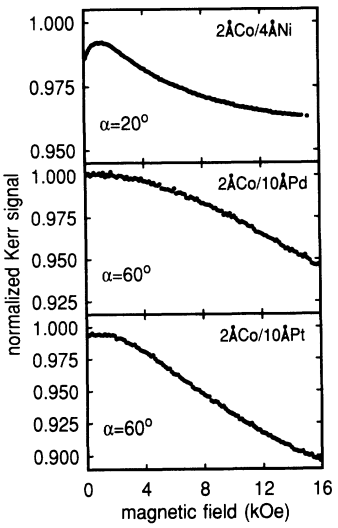

FIG. 3. Normalized polar Kerr measurements at field angle α with respect to the normal direction in the $0 \leq H \leq 16$ kOe range. The measurement geometry is analogous to the one in Fig. 1.

angle at a given field strength H and orientation α. This equilibrium is achieved when the external field torque $L(\alpha) = -\mu_0 M_S H \sin(\theta_{eq} - \alpha)$ is compensated by the internal torque due to the intrinsic magnetic anisotropies, $+[(K'_{u,1}+K_{u,2}) \sin 2\theta + \frac{1}{2} K_{u,2} \sin 4\theta]$. Least squares fits of field dependences, as shown in Fig. 3, yield the anisotropy fields

$$H'_{a,1} = \frac{2K'_{u,1} + 4K_{u,2}}{M_S}$$

and

$$H_{a,2} = \frac{4K_{u,2}}{M_S}, \tag{4}$$

which can be converted into the anisotropy constants $K_{u,1}$ and $K_{u,2}$ using the independently measured saturation magnetizations M_S and demagnetization energies K_d. In Table II we have summarized the most important results of the present Kerr studies. Quoted are first the saturation Kerr rotation θ_S, the coercivity H_C, and the remanence ratio r from measurements at a field angle $\alpha = 0°$ (columns 2–4). Columns 5 and 6 show the measured anisotropy fields $H'_{a,1}$ and $H_{a,2}$ as deduced from the results shown in Fig. 3. Columns 7 and 8 finally show the anisotropy constants $K_{u,1}$ and $K_{u,2}$, which were derived according to Eq. (4) with the use of the saturation magnetization data quoted in Table I. The $K_{u,1}$ values obtained from the Kerr analysis agree within 10–20 % with $K_\perp$, derived from the 45° torque analysis. Also, the appearance of higher-order anisotropy terms, $K_{u,2}$, is confirmed. We find it interesting to note that the ratio $K_{u,1}/K_{u,2}$ is approximately four in all cases, which is close to the ratio of three expected for bulk hcp Co.

For a detailed discussion of hysteresis properties of Co/Pt multilayers with buffers, we refer to the work of Lin *et al.*,[24] who used the same deposition system as in the present study. For more details on Co/Ni multilayers the reader is referred to the work of den Broeder *et al.*[25] The well-known strong dependence of the perpendicular magnetic anisotropy, coercivity, and remanence on the degree of (111) texturing in fact was exploited to fabricate structures with high perpendicular remanence, which is essential for the XMCD measurement scheme employed by us (*vide infra*).

IV. DICHROISM MEASUREMENTS

XMCD experiments were performed at the Stanford Synchrotron Radiation Laboratory (SSRL) on beamline 8-2 which is equipped with a spherical grating monochromator. Circularly polarized x rays were obtained by moving the prefocusing mirror below the electron orbital plane yielding a degree of circular polarization of 90±5 %. The XMCD signal is defined as the difference in absorption of right and left circularly polarized x rays near an atomic absorption edge. It can be measured (i) by changing the photon helicity for a fixed magnetization direction of the sample or (ii) by reversing the magnetization direction of the sample for a fixed photon helicity. We used the second approach and have detected the dichroism effect by measuring the absorption difference from two pieces of the same sample, which were premagnetized in opposite directions. Negligible magnetic stray fields allowed us to conveniently determine the x-ray absorption by total electron yield detection using a channeltron electron multiplier.[26] All multilayer samples were measured in a normal x-ray incidence geometry. For the Co film a glancing angle of 20° was chosen. In this latter case the experimentally derived moments were multiplied by a scaling factor of $1/\cos 20° = 1.06$ to correct for the misalignment of the photon propagation and magnetization direction.

The x-ray absorption spectra for the two opposite orientations of photon spin and magnetization direction

TABLE II. Magnetic properties of Co/Ni, Co/Pd, and Co/Pt multilayers obtained from polar Kerr loop measurements, θ_S, saturation Kerr rotation in deg; H_C, coercivity in kOe; r, remanence ratio; H'_a and H^2_a, effective and second-order anisotropy fields in kOe; $K_{u,1}$ and $K_{u,2}$, anisotropy constants derived according to Eq. (4) (in MJ/m^3).

Structure	θ_S	H_C	r	H'_a	H^2_a	$K_{u,1}$	$K_{u,2}$
Au(300)/20×[Co(2)/Ni(4)]	0.2618	0.51	0.94	-10.94	7.99	0.641	0.162
Pd(200)/20×[Co(2)/Pd(10)]	0.1162	5.61	0.99	-46.93	20.00	0.701	0.180
Pt(200)/20×[Co(2)/Pt(10)]	0.1495	4.31	0.97	-28.95	15.18	0.420	0.118

were converted into dichroism spectra by using the following analysis method. First, a constant background is subtracted which is determined by the intensity below the Co L_3 edge. Second, both spectra are renormalized to a constant edge jump, with the normalization constant determined from the data far above the Co L_2 edge. This procedure is based on the assumption that the size of the edge jump far from the absorption edge is independent of the local Co environment and is proportional to the number of Co atoms. The difference spectra are subsequently determined from these normalized individual absorption spectra and the dichroism intensities at the L_3 and L_2 edges are obtained by integrating over the respective peaks at these two edges.

V. EXPERIMENTAL RESULTS

Figure 4 shows results of normalized absorption (upper panel) and difference spectra (lower panel) of a pure Co film and the present multilayer samples with d_{Co}=2 Å. The arrow symbols refer to the photon spin parallel/antiparallel to the majority electron spin direction, which is opposite to the magnetization direction. Large differences are observed in both the individual and difference spectra. In particular, the spectra for Co in Co/Pd and Co/Pt exhibit very strong resonance ("white line") intensities as well as large amplitudes in the difference spectra. The spectra for Co in Co/Ni and in bulk Co show considerably smaller effects. A quantitative analysis of the data is presented in Table III. We have listed the integrated white line intensities $A^{+/-}_{L_{2/3}}$ for the two relative orientations as well as their differences (dichroism intensities) $\Delta A_{L_{2/3}}$ at both edges. Note that the white line intensities were obtained after subtracting a steplike background from the original data. Because of the uncertainty of this procedure the differences $(A^{+}_{L_{2,3}} - A^{-}_{L_{2,3}})$ differ from the values $\Delta A_{L_{2,3}}$ in Table III which were directly obtained from the difference spectra. The slightly reduced remanence ratios r, as listed in Table II, have not been corrected for in the spectra displayed in Fig. 4. They were, however, taken into account in evaluating the integrated white line and dichroism intensities listed in Table III.

The orbital moment sum rule introduced by Thole

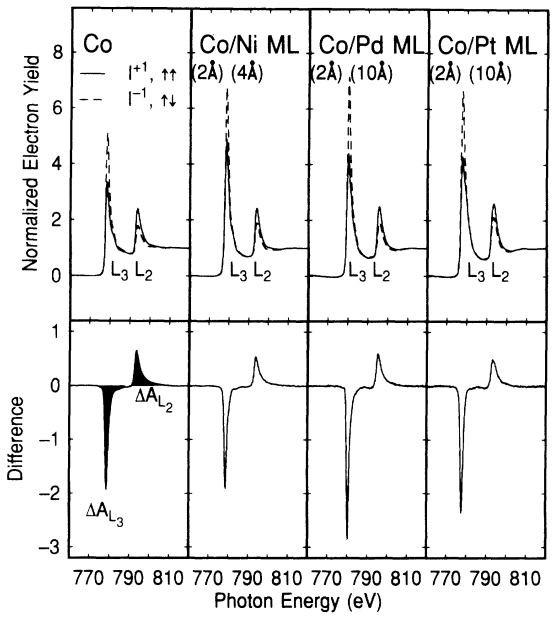

FIG. 4. Circularly polarized x-ray absorption spectra near the Co L_3(778 eV) and L_2(793 eV) edges for the two opposite relative orientations (parallel and antiparallel) of the photon spin and majority electron spin directions (upper panel) and their difference, the magnetic circular dichroism signal (lower panel) for Co in bulk Co and Co/Ni, Co/Pd, and Co/Pt multilayers.

et al.[27] and recently confirmed by Wu *et al.*[28] was used in conjunction with the analysis method suggested by Wu *et al.*[14] to determine the orbital magnetic moment: $m_{orb} = -\mu_B \langle L_Z \rangle / \hbar$. Note that the expectation value $\langle L_Z \rangle$ of the d electron moment is measured in units of $\hbar$ defined with respect to the spin quantization axis z (normal direction for the present multilayer samples) and has the opposite sign than the orbital moment m_{orb}, which is measured in units of Bohr magnetons, μ_B. The orbital moment is linked to the individual dichroism intensities according to

$$m_{orb} = C(\Delta A_{L_3} + \Delta A_{L_2}) = C \Delta A_T. \quad (5)$$

The proportionality constant C was determined by us-

TABLE III. Measured XMCD intensities and derived Co orbital moments for Co in a Co thin film and Co in Co/Ni, Co/Pd, and Co/Pt multilayers. The difference intensities were obtained by integrating over the intensities in the difference spectra (see text). A comparison to calculated orbital Co d moments (Ref. 29) and the experimentally derived intrinsic anisotropy constants $K^{Co}_{u,1} = K_{u,1} D/d_{Co}$ (in MJ/m^3 per Co volume) is given in the last two columns.

	$A^{+}_{L_3}$	$A^{-}_{L_3}$	$A^{+}_{L_2}$	$A^{-}_{L_2}$	ΔA_{L_3}	ΔA_{L_2}	ΔA_T	$(m^{\perp}_{orb})\|_{expt}$	$(m^{\perp}_{orb})\|_{calc}$[a]	$K^{Co}_{u,1}$
Co	7.4	11.3	4.9	2.6	-4.4	2.4	-2.0	0.14[b]	0.13[b]	0.45[c]
Co/Ni	11.4	15.1	4.3	2.7	-4.0	2.1	-1.9	0.13	0.13	1.92
Co/Pd	11.9	17.2	5.0	2.8	-6.4	2.3	-4.1	0.29	0.28	4.21
Co/Pt	14.9	20.1	5.9	4.4	-5.0	1.9	-3.0	0.21	0.20	2.52

[a]From Ref. 29.
[b]$m^{\perp}_{orb} \approx m^{\parallel}_{orb}$ in bulk Co (Ref. 6).
[c]K_1 from Ref. 15.

ing Co metal as a standard. We obtain $C = -0.07\mu_B$ by using the value $m_{\rm orb} = 0.14\mu_B$ ($\langle L_Z \rangle = -0.14\hbar$) for Co metal.[8] We note that the value of the proportionality constant C is sensitive to the degree of circular polarization of the x rays and to the data analysis procedure, and therefore a consistent procedure has to be used for all data. We also note that we have ignored any anisotropies in the orbital d moment of bulk Co. Such anisotropies are weak and in the order of $\sim 0.01\mu_B$,[6] which is below the accuracy limit of the present measurement.

We find that Co in Co/Ni and bulk Co have the same orbital moment within the experimental error of $\sim \pm 0.02\mu_B$ in the present case. The orbital moment of Co in Co/Pd is strongly enhanced, as reported before[14] and Co in Co/Pt also shows a strong, but slightly smaller enhancement. These results are in excellent agreement, both in trend and absolute magnitude, with theoretical values of Daalderop *et al.*,[4,29] who predicted orbital magnetic moment enhancements in several multilayer and ordered compound systems. This comparison, which is included in Table III, therefore generally supports their theory. The quantitative agreement of the absolute moment values between this theory and our experimental results may, however, be somewhat fortuitous because the structures underlying the *ab initio* calculations[4] have abrupt interfaces, coherent lattices and vanishing interdiffusion. The measured samples on the other hand are polycrystalline films with defects and, quite likely, graded and chemically intermixed interfaces. Note also that the theoretical value for the orbital magnetic moment depends on the details of the band-structure calculation and, in particular, on the inclusion of an orbital polarization term, which is needed to account for the experimentally observed orbital moment of $0.14\mu_B$ in bulk hcp Co.[8,3] Without this term, values in the order of only $\sim 0.08\mu_B$ for Co are found.[8,30] We finally note that although the quoted theoretical values represent total orbital moments the contributions from s, p, and f electrons are negligibly small such that the calculated moments can be directly compared to the experimental values, which are pure d moments.

VI. DISCUSSION

We now return to the question of a possible correlation between the orbital magnetic moment enhancement and the intrinsic uniaxial anisotropy. First we renormalize the $K_{u,1}$ data, which are averaged values over the total sample volume, as quoted in Table II, to the Co volume only according to $K_{u,1}^{\rm Co} = K_{u,1} D/d_{\rm Co}$. By doing so, we make the assumption that mainly Co atoms contribute to the anisotropy, which introduces a certain error, since Ni, Pd, and Pt atoms are also expected to contribute. The actual error that is introduced by this method may be estimated to be about 5–10% by comparing the averaged magnetizations M_S^X within the spacers Ni, Pd, and Pt to the magnetization $M_S^{\rm Co}$ within the Co layers. The actual comparison of the measured out-of-plane orbital moment $m_{\rm orb}^{\perp}$ and the uniaxial anisotropy constant $K_{u,1}^{\rm Co}$ (per Co volume) is shown in the last two columns of Table III

We find the interesting result plotted in Fig. 5, that the out-of-plane orbital Co d moments of Co/Ni, Co/Pd, and Co/Pt scale with the intrinsic first order anisotropy constants $K_{u,1}^{\rm Co}$ of these structures. This is quite surprising if one views the situation in bulk Fe, Co, and Ni, where typical intrinsic (magnetocrystalline) anisotropy constants K_1 of 0.5 in hcp Co, 0.05 in bcc Fe, and 0.005 in fcc Ni have been measured at room temperature (in MJ/m^3).[15] This variation by two orders of magnitude is in contrast to the change of the experimental orbital magnetic moments by only a factor of about 3, from 0.14 in Co to 0.08 in Fe to 0.05 in Ni (in μ_B).[5,8] Thus there is clearly no such scaling relation between $m_{\rm orb}$ and $K_{u,1}$ in the bulk. The situation may, however, be different at interfaces and our data provide first experimental evidence for this. The correlation shown in Fig. 5 provides evidence that the orbital d moment enhancement in the perpendicular direction and the interface induced perpendicular magnetic anisotropy in these multilayer structures have a common electronic origin and are directly related to each other.

A close connection between the magnetocrystalline anisotropy and the orbital moment has been predicted for transition metal monolayers of Fe, Co, and Ni. In a simple model Bruno[31] derived a relation between the orbital magnetic moment $m_{\rm orb}$ and the spin-orbit energy $E_{\rm SO}$ to first order in $\sin^2\theta$:

$$m_{\rm orb} = m_{\rm orb}^{\perp} + (m_{\rm orb}^{\parallel} - m_{\rm orb}^{\perp}) \sin^2\theta$$

and

$$E_{\rm SO} = -\frac{1}{2}\frac{\xi}{2\mu_B}[m_{\rm orb}^{\perp} + (m_{\rm orb}^{\parallel} - m_{\rm orb}^{\perp}) \sin^2\theta]. \quad (6)$$

These can be combined to yield the anisotropy energy $\Delta E_{\rm SO} = E_{\rm SO}(\theta = 0°) - E_{\rm SO}(\theta = 90°)$, i.e., the energy difference for the magnetization aligned along the normal direction ($\perp$) and the in-plane direction ($\parallel$):

$$\Delta E_{\rm SO} = -\frac{1}{2}\frac{\xi}{2\mu_B}[m_{\rm orb}^{\perp} - m_{\rm orb}^{\parallel}]. \quad (7)$$

Bruno[9] also made quantitative predictions for the

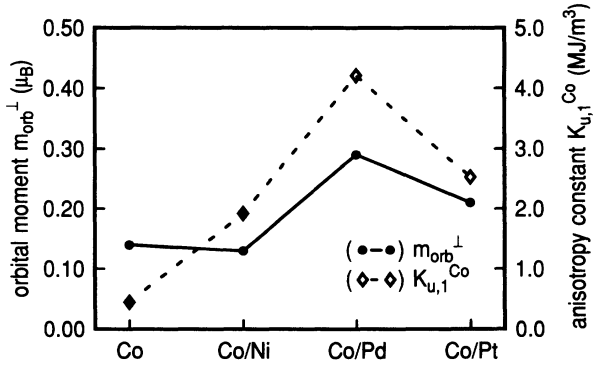

FIG. 5. Comparison of the measured out-of-plane orbital moment per Co atom $m_{\rm orb}^{\perp}$ (•) and the intrinsic magnetocrystalline anisotropy constant $K_{u,1}^{\rm Co}$ per Co volume (◇) in Co/Ni, Co/Pd, and Co/Pt multilayers with 2 Å Co thickness, and a thick Co reference film.

anisotropy of the orbital moment $\Delta m_{\rm orb} = | m^{\perp}_{\rm orb} - m^{\parallel}_{\rm orb} |$. For ultrathin freestanding monolayers he finds $\Delta m_{\rm orb}$ of the order of 0.1–0.2μ_B. These predictions were made using second-order perturbation theory, in which the spin-orbit energy is approximated by a one-electron term $E_{SO} = \xi_{SO}\, l{\cdot}\mathbf{s}$. Terms of higher than second order in $\sin\theta$ were neglected, which corresponds to the presently discussed uniaxial anisotropy case. The 3*d* and 4*s* bands were approximated by tight-binding calculations. Although we have not measured the above *anisotropy* of $m_{\rm orb}$, but only $m_{\rm orb} = m^{\perp}_{\rm orb}$, we find that the presently observed orbital moment enhancement, which we define as

$$\Delta m_{\rm orb} = (m^{\perp}_{\rm orb})|_{{\rm Co}/X} - (m_{\rm orb})|_{\rm Co,bulk}, \tag{8}$$

is in its magnitude consistent with Bruno's prediction. Thus it appears that the *enhancement* of $m^{\perp}_{\rm orb}$ in multilayers over the $m_{\rm orb}$ value for bulk Co is essentially proportional to the *anisotropy* of $m_{\rm orb}$. This would require the orbital moment enhancement according to Eq. (8) to be anisotropic, with a significantly smaller value parallel to the surface, i.e., $m^{\perp}_{\rm orb} > m^{\parallel}_{\rm orb} \approx m^{\rm bulk}_{\rm orb}$. Or in other words, the orbital moment enhancement would be strongly confined to the sample normal direction. We can in fact view our finding of a roughly linear scaling between $m^{\perp}_{\rm orb}$ and $K^{\rm Co}_{u,1}$ together with the result of Eq. (7) as experimental evidence for such an *anisotropic* enhancement of the orbital moment.

Bruno[9] also showed that there is a direct connection between the spin-orbit induced (magnetocrystalline) anisotropy and the spin-orbit coupling parameter ξ_{SO} for *d* electrons according to

$$K_{u,1} \propto \frac{\xi^2_{SO}}{W}, \tag{9}$$

where W represents the *d*-band width. In multilayers both ξ_{SO} and W of Co are expected to be affected by the adjacent spacer atoms if *d*-*d* mixing (hybridization, orbital overlap) is present. A strong influence of the spacer in establishing perpendicular magnetic anisotropy has indeed been predicted, due to *d*-*d* mixing,[32] in systems containing Pd and Pt, which show a large Stoner-enhanced susceptibility, and experimental evidence for such a correlation between $K_{u,1}$ and $\xi^{\rm Pd,Pt}_{SO}$ has recently been reported in Co-Pd and Co-Pt alloys[33] where the larger perpendicular magnetic anisotropy in Co-Pt compared to Co-Pd alloys was attributed to the larger spin-orbit coupling of Pt-5*d* electrons.

Our present results are consistent with the notion that *d*-*d* mixing between Co-3*d* and Pd-4*d* and Pt-5*d* states, respectively, leads to the observed large anisotropies and orbital moments, however, there is clearly no simple correlation, e.g., to ξ_{SO} of Ni, Pd, and Pt, as Eq. (9) might suggest. Note that the *d*-electron spin-orbit coupling parameters ξ_{SO} of Ni-3*d*, Pd-4*d*, and Pt-5*d* levels are about 100, 200, and 600 meV,[34] respectively, and clearly do *not* correlate with $K_{u,1}$ and/or $m^{\perp}_{\rm orb}$. The *d*-band width which enters the denominator in Eq. (9), on the other hand, is smaller in Pd systems than in Pt systems,[35] consistent with the observed larger $K_{u,1}$ value for Co/Pd.

Returning to the issue of the interfacial origin of the orbital moment enhancement, we note that phenomenologically, the anisotropy has been expressed in terms of an additional magnetocrystalline anisotropy term $2K_S/d_{\rm Co}$, which depends on the magnetic layer thickness—$d_{\rm Co}$ in this case—and can lead to a perpendicular easy axis in these films.[2,1] A similar strong dependence of the interface related *orbital moment enhancement* $\Delta m_{\rm orb}$, as defined in Eq. (8), might analogously be expected. It is therefore interesting to address the question on how rapidly the orbital moment decays back to the bulk Co value as the Co thickness increases. Roughly, a $1/d_{\rm Co}$ dependence might be expected if a one-to-one correlation existed. This behavior is, however, *not* observed for Co/Pd multilayers as shown in Fig. 6. The data were linearly rescaled for the nonunity remanence, which decreases rapidly as the Co layer thickness increases. The derived quantities therefore represent the measured orbital moment projected along the film normal divided by the remanent moment along that direction. Similar results are found for Co/Pt (not shown). Basically we find a constant orbital moment with an average value of $\bar{m}^{\perp}_{\rm orb} = 0.26\mu_B$ as indicated by the dotted line. The error bars in these measurements were estimated to be $\pm 0.04\mu_B$, which prohibit us from drawing any further conclusions on a possible thickness dependence over the investigated range.

The failure to find a $1/d_{\rm Co}$ or other functional dependence on the Co thickness shows that $\Delta m_{\rm orb}$ persists to at least two monolayers on each side of the interface. This may simply be due to the presence of intermixed, graded interfaces. Orbital magnetic moment enhancements of Co atoms diluted in Pd, as would be present in mixed interface regions, are well known in the literature and were already discussed in the mid 70s based on the observation of line broadening effects in nuclear magnetic resonance (NMR) experiments.[36,37]

Our experimental data are in good quantitative agreement with *ab initio* magnetocrystalline energy calculations of Daalderop *et al.*,[3] who conclude that in the

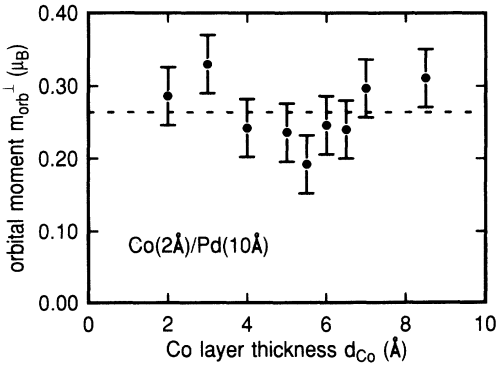

FIG. 6. Out-of-plane orbital moment, $m^{\perp}_{\rm orb}$, in the *d* shell of C atoms in the film normal direction as a function of the Co layer thickness in Co/Pd multilayers. The error bars are $\pm 0.04\mu_B$ in this particular measurement. The dotted line represents the mean value of $\bar{m}^{\perp}_{\rm orb}$=$0.26\mu_B$ obtained by averaging the present data points.

present systems the perpendicular magnetization orientation is stabilized by an enhanced *anisotropy* of the orbital moment. As already pointed out earlier by Bruno,[9] they further argue[4] that the perpendicular anisotropy is related to the details of the band structure near the Fermi surface and, in particular, to the band filling such that there is a presence of crystal field split states with $d_{x^2-y^2}$ and d_{xy} character near the Fermi level. Partial occupation of these states is responsible for the existence of a net orbital moment with a preferential direction normal to the interface. The coupling of the spin moment to these orbital moments via spin-orbit interaction finally leads to the macroscopically observable magnetic anisotropy with perpendicular orientation of the magnetization, as outlined in the Introduction.

VII. CONCLUSIONS

In summary, we have demonstrated a large enhancement of the orbital magnetic d moment of Co atoms in Co/Pd and Co/Pt multilayers, compared with bulk Co and Co/Ni multilayers, using x-ray magnetic circular dichroism spectroscopy (XMCD). This enhancement scales linearly with the observed first-order uniaxial anisotropy constants $K_{u,1}^{\mathrm{Co}}$ in these multilayer structures, which is interpreted as evidence for a preferential out-of-plane enhancement of the orbital moment. The fact that the enhancement is independent of the Co thickness extending at least up to 8.5 Å in Co/Pd and Co/Pt multilayers indicates the presence of intermixed interfaces on this thickness scale. There is no obvious correlation between the orbital moment enhancement and the spin-orbit coupling parameters of Ni-3d, Pd-4d, and Pt-5d states. It will be interesting to investigate immiscible, nonintermixing systems in the future, which might unambiguously prove the interface origin of the orbital moment enhancement, reported here. Further it will be important to measure the actual anisotropy, i.e., angle dependence, of the orbital moment directly. This will allow a direct comparison to predictions from *ab initio* theories of in-plane and out-of-plane orbital moments in ultrathin films and multilayers.

ACKNOWLEDGMENTS

S. S. P. Parkin and K. Roche kindly designed and provided the Co thin film sample used in this experiment. We are grateful to G. H. O. Daalderop for communicating theoretical results prior to publication and to P. Bagus and G. R. Harp for numerous discussions. We also acknowledge the help of M. Rowen and C. Troxel at SSRL. The work was carried out in part at SSRL which is operated by the Department of Energy, Division of Chemical Sciences. Institut d'Electronique Fondamentale is Unité Associée au CNRS No. 22.

[1] L. Néel, J. Phys. Radium **15**, 225 (1954).
[2] F. J. A. den Broeder, W. Hoving, and P. J. H. Bloemen, J. Magn. Magn. Mater. **93**, 562 (1991).
[3] G. H. O. Daalderop, P. J. Kelly, and M. F. H. Schuurmans, Phys. Rev. B **42**, 7270 (1990); **44**, 12054 (1992).
[4] G. H. O. Daalderop, P. J. Kelly, and F. J. A. den Broeder, Phys. Rev. Lett. **68**, 682 (1992).
[5] E. P. Wohlfahrt, in *Ferromagnetic Materials*, edited by E. P. Wohlfahrt (North-Holland, Amsterdam, 1980), Vol. 1.
[6] J.-P. Rebouillat, IEEE Trans. Magn. **8**, 630 (1972); R. Pauthenet, J. Appl. Phys. **53**, 8187 (1982); an anisotropy of the Co moment of $0.007\mu_B$, which is about 0.5% of the total moment is reported.
[7] M. B. Stearns, in *Numerical Data and Functional Relationships in Science and Technology*, edited by H. P. J. Wijn, Landolt-Börnstein, New Series, Group 3, Vol. 19 (Springer, Berlin, 1986).
[8] O. Eriksson, B. Johansson, R. C. Albers, A. M. Boring, and M. S. S. Brooks, Phys. Rev. B **42**, 2707 (1990); P. Söderlind, O. Eriksson, B. Johansson, R. C. Albers, and A. M. Boring, *ibid.* **45**, 12911 (1992).
[9] P. Bruno, Phys. Rev. B **39**, 865 (1989); Ph.D. thesis, Université de Paris-Sud, 1989 (unpublished).
[10] K. Kyuno, R. Yamamoto, and S. Asano, J. Phys. Soc. Jpn. **61**, 2099 (1992).
[11] D. Wang, R. Wu, and A. J. Freeman, Phys. Rev. Lett. **70**, 869 (1993).
[12] R. H. Victora and J. M. MacLaren, Phys. Rev. B **47**, 11583 (1993); J. M. MacLaren and R. H. Victora, IEEE Trans. Magn. **29**, 3034 (1993).
[13] S. Pick and H. Dreyssé, Phys. Rev. B **48**, 13588 (1993).
[14] Y. Wu, J. Stöhr, B. Hermsmeier, M. G. Samant, and D. Weller, Phys. Rev. Lett. **69**, 2307 (1992).
[15] B. D. Cullity, *Introduction to Magnetic Materials* (Addison-Wesley, Reading, MA, 1972).
[16] See, e.g., several papers in Proceedings of the E-MRS Spring Meeting, Strassbourg, 1990 [J. Magn. Magn. Mater. **93** (1991)].
[17] A large magnetic polarization has directly been observed in XMCD measurements of Pt spacers in Co/Pt multilayers by R. Wienke, G. Schütz, and H. Ebert, J. Appl. Phys. **69**, 6147 (1991); G. Schütz, H. Ebert, P. Fischer, S. Rüegg, and W. B. Zeper, in *Magnetic Thin Films, Multilayers, and Surfaces*, edited by S. S. P. Parkin, MRS Symposia Proceedings No. 231 (Materials Research Society, Pittsburgh, 1992), p. 77; and of Pd spacers in Co/Pd multilayers by D. Weller, Y. Wu, J. Stöhr, B. D. Hermsmeier, and M. G. Samant (unpublished).
[18] H. Ebert, S. Rüegg, G. Schütz, R. Wienke, and W. B. Zeper, J. Magn. Magn. Mater. **93**, 601 (1991).
[19] R. H. Victora and J. M. MacLaren, J. Appl. Phys. **69**, 5653 (1991).
[20] Te-ho Wu, Hong Fu, R. A. Haijjar, T. Suzuki, and M. Mansuripur, J. Appl. Phys. **73**, 1368 (1993).
[21] H. Miyajima, K. Sato, and T. Mizoguchi, J. Appl. Phys. **47**, 4669 (1976).

[22] R. A. Haijar, F. L. Zhou, and M. Mansuripur, J. Appl. Phys. **67**, 5328 (1990).
[23] S. T. Purcell, M. T. Johnson, N. W. E. McGee, W. B. Zeper, and W. Hoving, J. Magn. Magn. Mater. **113**, 257 (1992).
[24] C. J. Lin, G. L. Gorman, C. H. Lee, R. F. C. Farrow, E. E. Marinero, H. V. Do, H. Notarys, and C. J. Chien, J. Magn. Magn. Mater. **93**, 194 (1991).
[25] F. J. A. den Broeder, E. Janssen, W. Hoving, and W. B. Zeper, IEEE Trans. Magn. **28**, 2760 (1992).
[26] J. Stöhr, *NEXAFS Spectroscopy* (Springer, Heidelberg, 1992).
[27] B. T. Thole, P. Carra, F. Sette, and G. van der Laan, Phys. Rev. Lett. **68**, 1943 (1992).
[28] Ruqian Wu, Dingsheng Wang, and A. J. Freeman, Phys. Rev. Lett. **71**, 3581 (1993).
[29] G. H. O. Daalderop (private communication).
[30] J. Sticht (private communication).
[31] P. Bruno, *Physical Origins and Theoretical Models of Magnetic Anisotropy* (Ferienkurse des Forschungszentrums Jülich, Jülich, 1993).
[32] G. H. O. Daalderop, P. J. Kelly, and M. F. H. Schuurmans, Phys. Rev. B **41**, 11919 (1990).
[33] D. Weller, H. Brändle, and C. Chappert, J. Magn. Magn. Mater. **121**, 461 (1993).
[34] A. R. Mackintosh and O. K. Anderson, in *Electrons at the Fermi Surface*, edited by M. Springford (Cambridge University Press, Cambridge, 1980), p. 185.
[35] S. Hüfner and G. K. Wertheim, Phys. Lett. **47A**, 349 (1974); H. Höchst, S. Hüfner, and A. Goldmann, *ibid.* **57A**, 265 (1976).
[36] L. D. Khoi, P. Veillet, and I. A. Cambell, J. Phys. F **6**, L197 (1976).
[37] S. Senoussi, I. A. Campbell, and A. Fert, Solid State Commun. **21**, 269 (1977).